Supporting information

Ground-based MAX-DOAS observations of tropospheric ozone and its precursors for diagnosing ozone formation sensitivity

Yuanyuan Qian[1, 3], Dan Wang[1, 3], Zhiyan Li[1, 3], Ge Yan[2], Minjie Zhao[3], Haijin Zhou[3], Fuqi Si[3] and Yuhan Luo[3, *]

1. School of Microelectronics & Data Science, Anhui University of Technology, Maanshan, 243032, China
2. Jianghuai Advanced Technology Center, Hefei, 230088, China
3. Key Laboratory of Environmental Optics & Technology, Anhui Institute of Optics and Fine Mechanics, Hefei Institutes of Physical Science, Chinese Academy of Sciences, Hefei, 230031, China

---

* Corresponding authors. E-mail: yhluo@aiofm.ac.cn (Yuhan Luo)

Text S1. DOAS method for retrieving DSCDs of trace gases

Differential optical absorption spectroscopy (DOAS) is an optical remote sensing technique that can identify trace gas concentrations by separating narrow-band (differential absorptions) and broad-band structures. The basic DOAS equation can be expressed as follows:

$$I(\lambda) = I_o(\lambda) \bullet \exp\left\{-\int\left[\sum_{j=1}^{n}\left(\sigma_j^*(\lambda)+\sigma_j(\lambda)\right)\bullet c_j + \varepsilon_R(\lambda)+\varepsilon_M(\lambda)\right]dl\right\} \qquad (1)$$

Where $I(\lambda)$ and $I_o(\lambda)$ represent incident intensity and original intensity (solar intensity in this study) at wavelength λ respectively; σ_j^* and σ_j represent narrow-band and broad-band absorption cross sections of trace gas j respectively; c_j represents the averaged concentration of j; ε_R and ε_M (broad-band structures) represent the Rayleigh and Mie scatter coefficients respectively; and l represents the light path. We can define I^* as the intensity without differential absorption. Therefore, formula (1) can be transformed as follows:

$$\ln\frac{I^*(\lambda)}{I(\lambda)} = \int\left[\sum_{j=1}^{n}\sigma_j^*(\lambda)\bullet c_j\right]dl = \sum_{j=1}^{n}\left(\sigma_j^*(\lambda)\bullet \mathrm{SCD}_j\right) \qquad (2)$$

Where $\mathrm{SCD}_j = \int c_j \bullet dl$ represents slant column density (SCD), and $D' = \ln\frac{I^*(\lambda)}{I(\lambda)}$ represents the differential optical density. The corresponding SCDs can be retrieved by fitting D' using the least-squares method. The sequential zenith spectrum is generally used as the reference spectrum for DOAS fitting to eliminate Fraunhofer absorption, thus obtaining the differential SCD (DSCD):

$$DSCD(\alpha) = SCD(\alpha) - SCD(90^\circ) \qquad (3)$$

Where α denotes the off-zenith elevation angles.

Table S1. The detailed parameters of DOAS fitting for O_4, NO_2, and HCHO.

Parameter	Data source	Trace gases			
		NO_2	**HCHO**	**O_3**	**O_4**
Fitting Interval (nm)		338–370	336.5–359	320–340	338–370
Polynomial order	5	√	√	√	√
Offset	Constant	√	√	√	√
O_3	223 K, 293 K (Bogumil et al.,2003)	√	√	√	√
NO_2	298 K (Vandaele et al., 1996)	√	√	√	√
O_4	293 K (Thalman and Volkmer, 2013)	√	√	√	√
HCHO	297 K (Meller and Moortgat, 2000)	√	√	√	√
BrO	223 K (Fleischmann et al., 2004)	√	√	√	√
Ring	Calculated using Ring.exe	√	√	√	√

Table S2. The detailed regime transitions and contributions of VOC-limited, NO_x-limited, and VOC-NO_x-limited regimes at lowest 1 km.

Height (km)	R	Polynomial	Peak	Regime transition	VOC-limited (%)	NO_x-limited (%)	VOC-NO_x-limited (%)
0–0.1	0.69	$y=59.8+43.9x+4.8x^2-4.1x^3$	2.33	2.21–2.46	87.47	7.59	4.94
0.1–0.2	0.67	$y=30.1+103.4x-23.4x^2+1.5x^3$	3.22	3.01–3.44	80.82	11.34	7.84
0.2–0.3	0.66	$y=63.2+105x-16.9x^2+0.5x^3$	3.78	3.49–4.06	66.15	26.09	7.76
0.3–0.4	0.62	$y=75+77.7x-12.3x^2+0.6x^3$	4.33	3.90–4.79	59.08	31.29	9.63
0.4–0.5	0.58	$y=77.8+52.3x-7.6x^2+0.3x^3$	4.70	4.27–5.15	55.33	33.76	10.91
0.5–0.6	0.53	$y=117.7+1.8x+0.4x^2-0.1x^3$	4.96	4.43–5.47	57.03	30.69	12.28
0.6–0.7	0.56	$y=88.3+12.6x+0.2x^2-0.2x^3$	5.54	5.08–5.97	72.89	18.50	8.61
0.7–0.8	0.50	$y=70.5-22x+11.9x^2-1.1x^3$	5.77	5.38–6.14	85.93	8.95	5.12
0.8–0.9	0.49	$y=40.2+0.8x+7.6x^2-1.1x^3$	4.72	4.41–5.01	88.49	8.53	2.98
0.9–1.0	0.51	$y=57.3-31.6x+24.9x^2-3.8x^3$	3.66	3.42–3.89	88.66	8.10	3.24

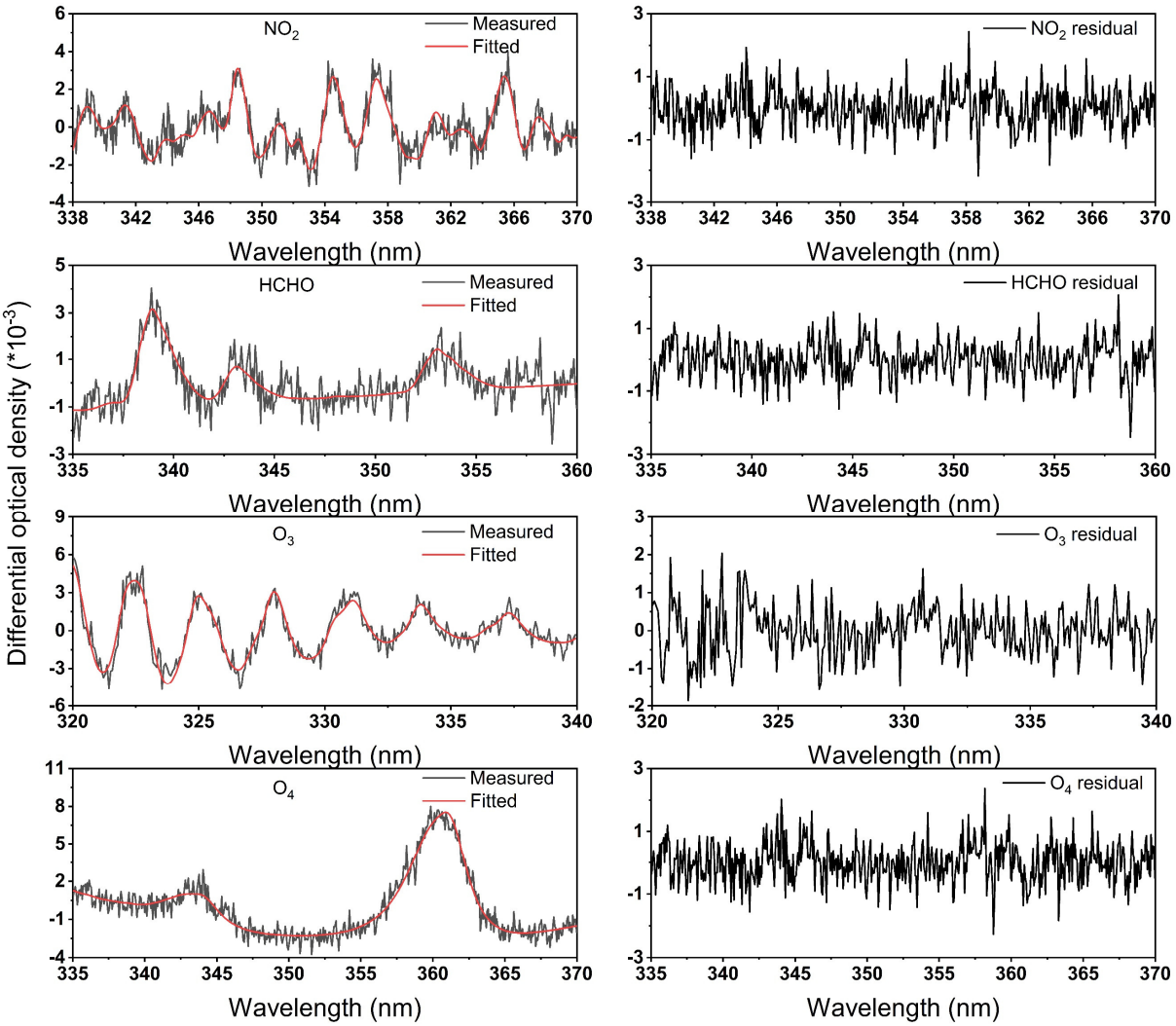


Fig. S1. An example of typical spectral fitting.

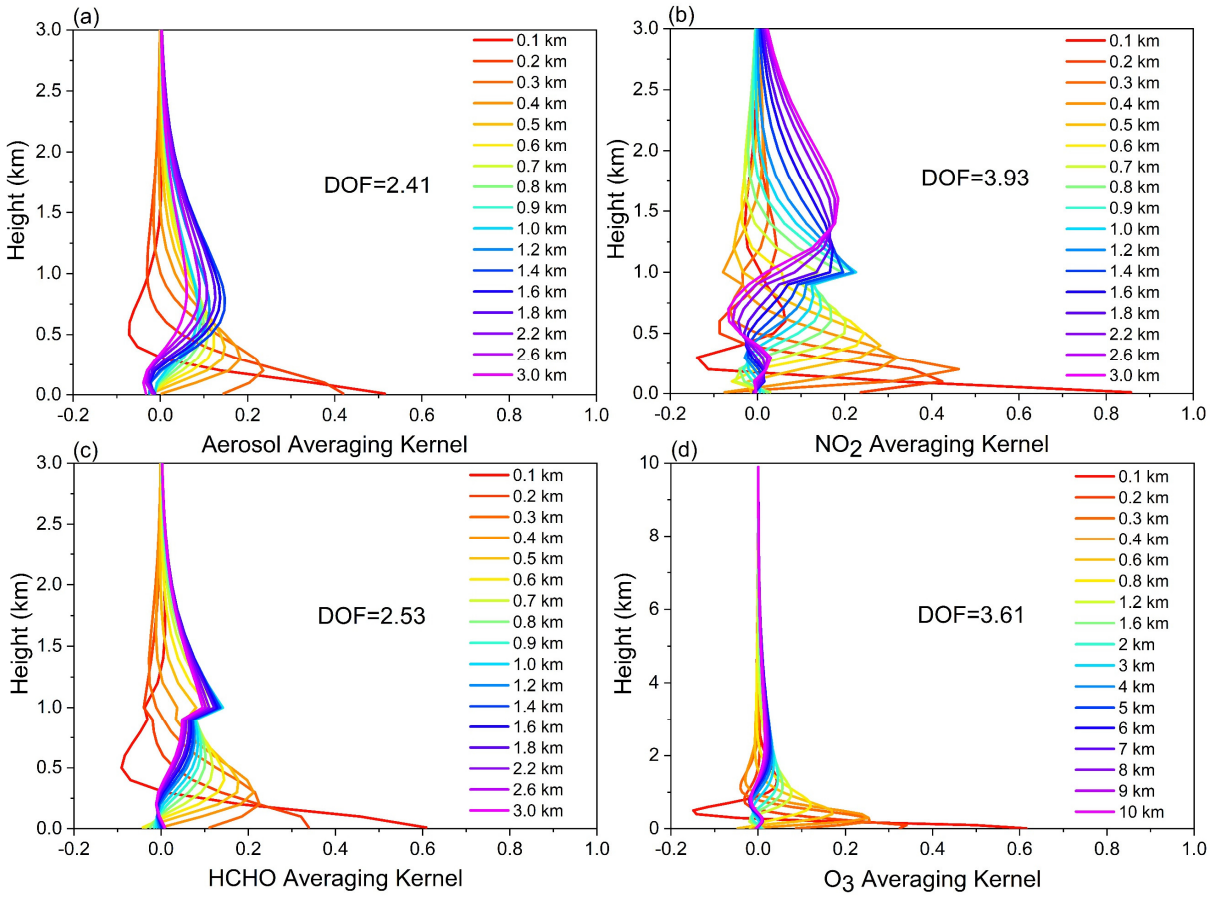


Fig. S2. The typical averaging kernels of aerosol (a), NO_2 (b), HCHO (c), and O_3 (d) retrievals.

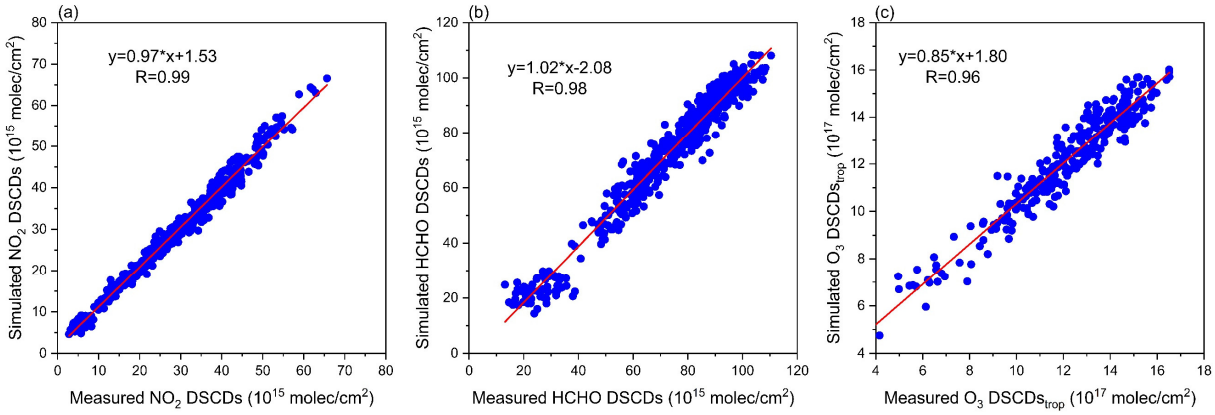


Fig. S3. Linear regression analyses between measured and simulated DSCDs of NO_2 (a), HCHO (b), and O_3 (c).

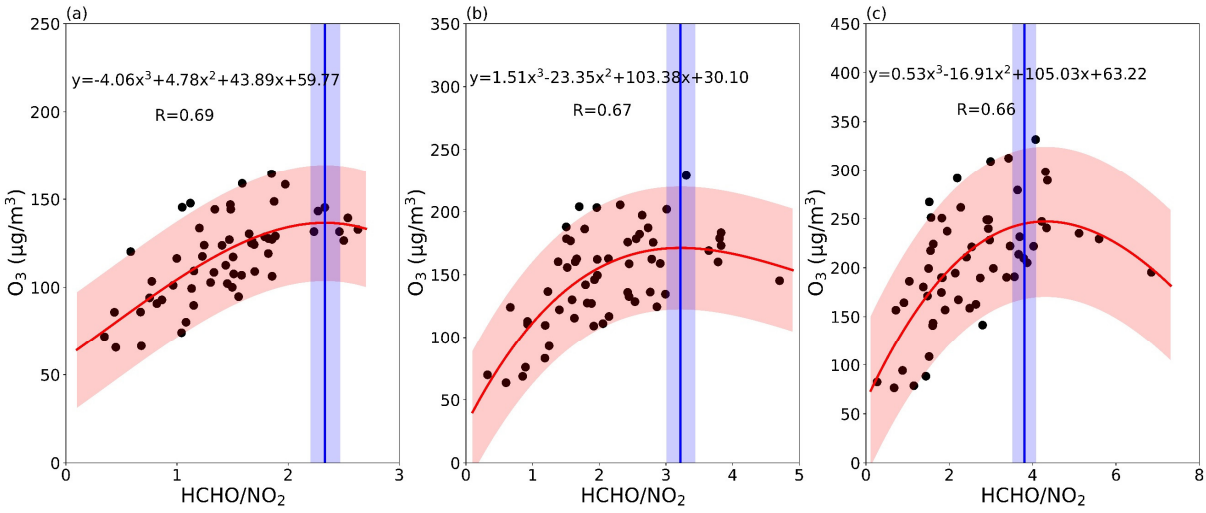


Fig. S4. Regime transitions of 0–0.1 km (a), 0.1–0.2 km (b), and 0.2–0.3 km (c).

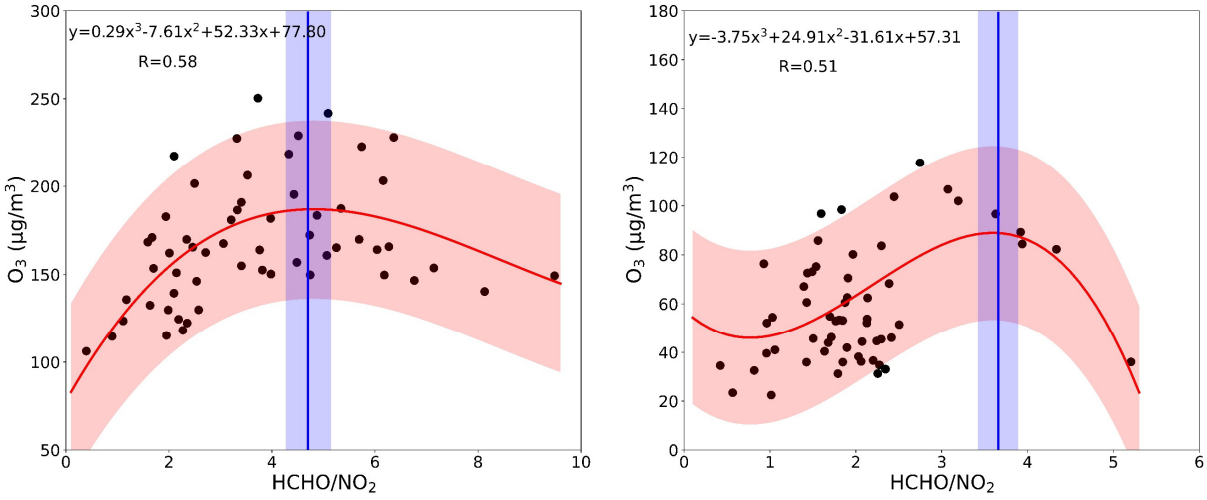


Fig. S5. Regime transitions of mid-layer (0.4–0.5 km, left panel) and top-layer (0.9–1.0 km, right panel).

Reference

Bogumil, K., Orphal, J., Homann, T., Voigt, S., Spietz, P., Fleischmann, O.C., Vogel, A., Hartmann, M., Kromminga, H., Bovensmann, H., Frerick, J., Burrows, J.P., 2003. Measurements of molecular absorption spectra with the SCIAMACHY pre-flight model: instrument characterization and reference data for atmospheric remote-sensing in the 230-2380 nm region. J. Photochem. Photobiol. A Chem. 157, 167-184. https://doi.org/10.1016/S1010-6030(03)00062-5

Fleischmann, O.C., Hartmann, M., Burrows, J.P., Orphal, J., 2004. New ultraviolet absorption cross-sections of BrO at atmospheric temperatures measured by time-windowing Fourier transform spectroscopy. J. Photochem. Photobiol. A Chem. 168, 117-132. https://doi.org/10.1016/j.jphotochem.2004.03.026

Meller, R., Moortgat, G.K., 2000. Temperature dependence of the absorption cross sections of formaldehyde between 223 and 323 K in the wavelength range 225-375 nm. J. Geophys. Res. 105, 7089-7101. https://doi.org/10.1029/1999JD901074

Thalman, R., Volkamer, R., 2013. Temperature dependent absorption cross-sections of O_2-O_2 collision pairs between 340 and 630 nm and at atmospherically relevant pressure. Phys. Chem. Chem. Phys. 15, 15371-15381. https://doi.org/10.1039/C3CP50968K

Vandaele, A.C., Hermans, C., Simon, P.C., Van Roozendaele, M., Guilmot, J.M., Carleer, M., Colin, R., 1996. Fourier transform measurement of NO_2 absorption cross-section in the visible range at room temperature. J. Atmos. Chem. 25, 289-305. https://doi.org/10.1007/BF00053797